fractal and fractional

MDPI

Article

An Effective Iterative Process Utilizing Transcendental Sine Functions for the Generation of Julia and Mandelbrot Sets

Khairul Habib Alam [1,*], Yumnam Rohen [2], Anita Tomar [3], Naeem Saleem [4,5,*], Maggie Aphane [5] and Asima Razzaque [6,7]

[1] Department of Mathematics, National Institute of Technology Manipur, Imphal 795004, Manipur, India
[2] Department of Mathematics, Manipur University, Imphal 795003, Manipur, India
[3] Pt. L. M. S. Campus, Sridev Suman Uttarakhand University, Rishikesh 249201, Uttarakhand, India
[4] Department of Mathematics, University of Management and Technology, Lahore 54770, Pakistan
[5] Department of Mathematics and Applied Mathematics, Sefako Makgatho Health Sciences University, Pretoria 0204, South Africa
[6] Department of Basic Sciences, Preparatory Year, King Faisal University, Al-Ahsa 31982, Saudi Arabia; arazzaque@kfu.edu.sa
[7] Department of Mathematics, College of Science, King Faisal University, Al-Ahsa 31982, Saudi Arabia
* Correspondence: alamkh@nitmanipur.ac.in (K.H.A.); naeem.saleem2@gmail.com (N.S.)

Abstract: This study presents an innovative iterative method designed to approximate common fixed points of generalized contractive mappings. We provide theorems that confirm the convergence and stability of the proposed iteration scheme, further illustrated through examples and visual demonstrations. Moreover, we apply s-convexity to the iteration procedure to construct orbits under convexity conditions, and we present a theorem that determines the condition when a sequence diverges to infinity, known as the escape criterion, for the transcendental sine function $\sin(u^m) - \alpha u + \beta$, where $u, \alpha, \beta \in \mathbb{C}$ and $m \geq 2$. Additionally, we generate chaotic fractals for this orbit, governed by escape criteria, with numerical examples implemented using MATHEMATICA software. Visual representations are included to demonstrate how various parameters influence the coloration and dynamics of the fractals. Furthermore, we observe that enlarging the Mandelbrot set near its petal edges reveals the Julia set, indicating that every point in the Mandelbrot set contains substantial data corresponding to the Julia set's structure.

Keywords: efficiency; stability; escape criterion; fractals; Julia set; Mandelbrot set; s-convexity

MSC: 28A10; 31E05; 37C25; 37F46; 47H10; 47J25

Academic Editors: María A. Navascués, Cristina Serpa and Bilel Selmi

Received: 2 December 2024
Revised: 3 January 2025
Accepted: 7 January 2025
Published: 15 January 2025

Citation: Alam, K.H.; Rohen, Y.; Tomar, A.; Saleem, N.; Aphane, M.; Razzaque, A. An Effective Iterative Process Utilizing Transcendental Sine Functions for the Generation of Julia and Mandelbrot Sets. *Fractal Fract.* **2025**, *9*, 40. https://doi.org/10.3390/fractalfract9010040

1. Introduction

Fixed point theory, a growing branch of mathematics, combines functional analysis and topology (see [1,2]). Specific iterative methods, such as those by Picard [3], Mann [4], Ishikawa [5], and Noor [6], are commonly employed to approximate fixed points of contractive mappings. Recent advancements include the application of Fibonacci–Ishikawa iteration for solving Caputo-type nonlinear fractional differential equations involving monotone asymptotically non-expansive mappings by Alam et al. [7] and their study [8] addressing nonlinear integral equations with two delays in hyperbolic spaces. Furthermore, Alam [9] introduced an efficient iterative approach for fractional Volterra–Fredholm integro-differential equations. Ofem et al. [10] proposed the AI iteration method, which improves the speed of fixed-point approximations.

Furthermore, numerous researchers have proposed the use of s-convexity in their studies (see, [11–15]). These diverse iteration processes can be examined from two perspectives. Firstly, they generally achieve faster convergence compared to traditional iterative methods. Secondly, each iteration method displays distinct dynamics and behaviors, which are valuable from both application and graphical viewpoints.

Fractals, characterized by their self-similar structures across scales, have had a profound impact on fields like art, physics, biology, and finance [16–19]. The advent of computational graphics during the "Fractals Era" at the end of the 20th century brought fractals, such as the Mandelbrot set [20,21] and the Julia set [22,23], into prominence. These sets are generated using iterative processes on complex numbers, revealing intricate visual patterns. The applications of fractals extend to image compression [24], signal processing [25], data compression [26], and human body organs [27], and their aesthetic appeal has inspired the field of fractal art [28]. Theoretical studies of fractals continue in geometry, dynamical systems, and topology [14].

The Mandelbrot set has been generalized using functions like $u^m + \beta$ instead of quadratic polynomials [29,30] and further expanded to include elliptic, transcendental, and rational functions, as well as extensions to systems like octonions [31], bicomplex numbers, and quaternions. Cyclical techniques, such as superfractals [32], inversion fractals, v-variable fractals, and biomorphs [33], have been used to identify fixed points and construct fractals via fixed-point theory. Iterative methods, such as Mann [34], Ishikawa [35], and Jungck–Mann [36], have been applied to visualize Julia and Mandelbrot sets, often incorporating s-convexity to enhance these techniques [12,37]. Recently, Alam et al. [38] investigated the escape criterion for generating fractals as Julia and Mandelbrot sets via s-convex AI iteration for functions of the type $\cos(u^m) - \alpha u + \beta$.

Building on this foundation, we introduce the Jungck–AI iteration process, demonstrating its convergence and stability through examples and visualizations. We incorporate s-convexity into this process to generate fractals based on the transcendental sine function $\sin(u^m) - \alpha u + \beta$, establishing an escape criterion for this function and the associated orbit under convexity conditions. Using MATHEMATICA, we analyze the chaotic properties of these fractals and illustrate the effects of various parameters on their dynamics. The ability of fractal geometry to capture intricate real-world structures has transformative potential in fields like textile design (e.g., Batik and Kalamkari). Fractal-based design automation supports scalability, reduces errors, promotes global collaboration, and lowers costs, driving industry growth and sustainability.

Section 2 outlines key definitions and concepts essential for the analysis. Section 3 proves that iterative methods Jungck–S, Jungck–CR, and Jungck–DK converge slower than the proposed Jungck–AI iteration. A numerical example validates this and shows that the weak compatibility condition ensures a unique common fixed point for both contractions, where our iteration converges. Section 4 explores the escape criterion of the Jungck–AI orbit using s-convex combinations for transcendental sine functions in the complex plane. Using MATHEMATICA 12.3, we generate chaotic fractals, including Julia and Mandelbrot sets, on a system with an 11th Gen Intel i3-1115G4 processor, 8 GB RAM, and Windows 11. Section 5 concludes the study.

2. Preliminaries

This section provides key definitions and discusses related concepts that will be useful in our analysis. Let $T : A \longrightarrow A$ be a self-mapping within a Banach space A. The AI iteration process, as outlined in [10], is described as

$$\begin{cases} u_{n+1} = Tv_n \\ v_n = Tw_n \\ w_n = Tx_n \\ x_n = a_n Tu_n + (1 - a_n)u_n, \ n \in \mathbb{N}, \end{cases}$$

for random choice, $u_1 \in A$, where $\{a_n\} \subset [0, 1]$.

For two non-self mappings $S, T : B \longrightarrow A$, defined on a nonempty subset B of a Banach space A, where $T(A) \subseteq S(A)$, Jungck [39] introduced an iterative process satisfying the contraction condition:

$$d(Tu, Tv) \leq \lambda d(Su, Sv), \ \lambda \in [0, 1).$$

Chugh et al. [40] proposed the Jungck–SP iterative scheme, which is described as follows:

$$\begin{cases} Su_{n+1} = a_n Tv_n + (1 - a_n)Sv_n \\ Sv_n = b_n Tw_n + (1 - a_n)Sw_n \\ Sw_n = c_n Tu_n + (1 - c_n)Su_n, \ n \in \mathbb{N}, \end{cases} \tag{1}$$

for random choice, $u_1 \in B$, where $\{a_n\}, \{b_n\}, \{c_n\} \subset [0, 1]$.

Definition 1 ([41]). *Two non-self mappings $S, T : A \longrightarrow A$ on a nonempty Banach space A, with $T(A) \subseteq S(A)$, are said to satisfy a general contractive condition if*

$$||Tu - Tv|| \leq \varphi(||Su - Tu||) + \lambda||Su - Sv||, \ \forall \ u, v \in A$$

where $\lambda \in [0, 1)$ and $\varphi : (0, +\infty) \to (0, +\infty)$ is a monotonic function with $\varphi(0) = 0$.

Building on the general contractive condition outlined in [41], Hussain et al. [42] developed the Jungck–CR iteration process for sequences $\{a_n\}, \{b_n\}, \{c_n\} \subset [0, 1]$ as

$$\begin{cases} Su_{n+1} = a_n Tv_n + (1 - a_n)Sv_n \\ Sv_n = b_n Tw_n + (1 - a_n)Tu_n \\ Sw_n = c_n Tu_n + (1 - c_n)Su_n, \ n \in \mathbb{N}, \end{cases} \tag{2}$$

for random choice, $u_1 \in B$.

In recent work, Guran et al. [43] introduced the Jungck–DK iterative method for sequences $\{a_n\}, \{b_n\} \subset [0, 1]$ as

$$\begin{cases} Su_{n+1} = a_n Tv_n + (1 - a_n)Sw_n \\ Sv_n = b_n Tw_n + (1 - b_n)Su_n \\ Sw_n = Tu_n, \ n \in \mathbb{N}, \end{cases} \tag{3}$$

for random choice, $u_1 \in B$, and analyzed its efficiency compared to the iterative methods proposed by Chugh et al. [40] and Hussain et al. [42], as well as its stability and the escape criterion used for generating Mandelbrot and Julia sets.

Motivated by these considerations, we propose a new iteration procedure, referred to as the Jungck–AI, which demonstrates a faster convergence rate compared to the iterations introduced by Chugh et al. [40], Hussain et al. [42], and Guran et al. [43].

Our Jungck–AI iteration procedure is given by

$$\begin{cases} u_1 \in B \\ Su_{n+1} = Tv_n \\ Sv_n = Tw_n \\ Sw_n = Tx_n \\ Sx_n = a_n Tu_n + (1 - a_n)Su_n, \ \forall n \in \mathbb{N}, \end{cases} \tag{4}$$

for sequence $\{a_n\} \subseteq (0, 1)$.

Definition 2 ([44]). *Let $S, T : A \longrightarrow A$ be two mappings such that $Su = Tu$ for some $u \in A$. In this case, u is referred to as a coincidence point, and $Su = Tu = v$ is called a point of coincidence. If $Su = Tu = u$, then u is termed a common fixed point. Additionally, if $TSu = STu$ at a coincidence point u, the pair (S, T) is said to be weakly compatible.*

Definition 3 ([45]). *In any nonempty convex Banach space A, given a function F, a converging iteration procedure $Su_{n+1} = F(u_n, T)$ with $T(A) \subseteq S(A)$, which converges to a point of coincidence u, is said to be stable with respect to S and T or $(S, T)^{-}$stable if*

$$\lim_{n \to +\infty} ||S\gamma_n - F(\gamma_n, T)|| = 0 \Leftrightarrow \lim_{n \to +\infty} S\gamma_n = u,$$

for a chosen sequence $\{S\gamma_n\}$ in A.

Lemma 1 ([46]). *If for two real non-negative sequences $\{\gamma_n\}$ and $\{\delta_n\}$, we have $\gamma_{n+1} \leq (1 - \eta_n)\gamma_n + \delta_n$, where $0 < \eta_n < 1$, for all $n \in \mathbb{N}$, with $\sum_{n=0}^{\infty} \eta_n = \infty$ and $\lim_{n \to +\infty} \frac{\delta_n}{\eta_n} = 0$, then $\lim_{n \to +\infty} \gamma_n = 0$.*

Definition 4 ([22,23]). *A collection of complex numbers such that an orbit does not converge to an infinite point is a filled Julia set. If $T : \mathbb{C} \longrightarrow \mathbb{C}$ is a polynomial of degree $m(\geq 2)$, then the boundary set ∂F_T of the set $F_T = \{u \in \mathbb{C} : \{|T\, u_n|\}$ is bounded$\}$ is known as the Julia set.*

Definition 5 ([20,21]). *All of the parameter values β for which the filled-in Julia set of $T(u) = u^2 + \beta$ is connected to comprise the Mandelbrot set M. That is, $M = \{u \in \mathbb{C} : \partial F_T$ is connected$\}$ or $M = \{u \in \mathbb{C} : \{|T\, u_n|\} \nrightarrow +\infty$ whenever $n \to +\infty\}$.*

There are several generalizations of the convex combination in the literature; the s-convex combination is one example of such generalizations.

Definition 6 ([47]). *For a finite set of complex numbers $u_1, u_2, \ldots, u_n \in \mathbb{C}$, the s-convex combination is presented as $a_1^s u_1 + a_2^s u_2 + \cdots + a_n^s u_n$, where $0 \leq a_i \leq 1$ and $i \in \{1, 2, \ldots, n\}$ so that $\sum_{i=1}^{n} a_i = 1$.*

Let us observe that, for $s = 1$, the s-convex combination simplifies to the conventional convex combination.

3. Efficiency, Stability, and Convergence in an Arbitrary Banach Space

This section provides an analytical proof showing that the iterative sequences generated by Equations (1)–(3) converge at a slower rate compared to our Jungck–AI iteration procedure (4). We also include a numerical example to support our theoretical results. First, we demonstrate that the weak compatibility condition ensures the existence of a unique common fixed point for both contractions, to which our iteration (4) converges.

Theorem 1. *Let A be a Banach space, and $S, T : B \longrightarrow A$ be two non-self mappings that satisfy the general contractive condition, defined on a non-empty subset B such that $T(B) \subseteq S(B)$ and $S(B)$ is complete in A. Then, the Jungck–AI iteration procedure $\{Su_n\}$ defined in (4) converges strongly to the unique common fixed point $Sv = Tv = u$ (denoted as u) if S and T are weakly compatible and $A = B$.*

Proof. Initially, we show that the Jungck–AI iterative procedure (4) converges to u. Based on the definition of the Jungck–AI iteration procedure in (4), we derive four inequalities:

$$\begin{aligned} ||Su_{n+1} - u|| &= ||Tv_n - u|| \\ &= ||Tv_n - Tv|| \\ &\leq \varphi(||Sv - Tv||) + \lambda||Sv_n - Sv|| \\ &\leq \lambda||Sv_n - Sv|| \\ &= \lambda||Sv_n - u||, \end{aligned}$$

$$\begin{aligned} ||Sv_n - u|| &= ||Tw_n - u|| \\ &= ||Tw_n - Tv|| \\ &\leq \varphi(||Sv - Tv||) + \lambda||Sw_n - Sv|| \\ &\leq \lambda||Sw_n - Sv|| \\ &= \lambda||Sw_n - u||, \end{aligned}$$

$$\begin{aligned} ||Sw_n - u|| &= ||Tx_n - u|| \\ &= ||Tx_n - Tv|| \\ &\leq \varphi(||Sv - Tv||) + \lambda||Sx_n - Sv|| \\ &\leq \lambda||Sx_n - Sv|| \\ &= \lambda||Sx_n - u|| \end{aligned}$$

and

$$\begin{aligned} ||Sx_n - u|| &= ||a_nTu_n + (1 - a_n)Su_n - u|| \\ &\leq a_n||Tu_n - u|| + (1 - a_n)||Su_n - u|| \\ &= a_n||Tu_n - Tv|| + (1 - a_n)||Su_n - u|| \\ &\leq a_n(\varphi(||Sv - Tv||) + \lambda||Su_n - Sv||) + (1 - a_n)||Su_n - u|| \\ &\leq a_n\lambda||Su_n - Sv|| + (1 - a_n)||Su_n - u|| \\ &= a_n\lambda||Su_n - u|| + (1 - a_n)||Su_n - u|| \\ &= (1 - a_n(1 - \lambda))||Su_n - u||. \end{aligned}$$

Hence,

$$\begin{aligned} ||Su_{n+1} - u|| &\leq \lambda||Sv_n - u|| \\ &\leq \lambda^2||Sw_n - u|| \\ &\leq \lambda^3||Sx_n - u|| \\ &\leq \lambda^3(1 - a_n(1 - \lambda))||Su_n - u||. \end{aligned}$$

Since $1 - a_n(1 - \lambda) < 1$, we obtain

$$\begin{aligned} ||Su_{n+1} - u|| &\leq \lambda^3||Su_n - u|| \\ &\leq \lambda^6||Su_{n-1} - u|| \\ &\leq \lambda^{3n}||Su_1 - u||. \end{aligned}$$

Again, $0 < \lambda < 1$ implies $\lim_{n \to +\infty} ||Su_{n+1} - u|| = 0$; that is, the iteration procedure $\{Su_n\}$ defined in (4) converges to $Sv = Tv = u$.

We now prove that u is the unique common fixed point of S and T. Let u^* also be considered a point of coincidence. Consequently, v^* satisfies $Sv^* = Tv^* = u^*$. However, from the general contractive condition of S and T, we obtain the following

$$\begin{aligned} 0 \leq ||u - u^*|| &= ||Tv - Tv^*|| \\ &\leq \varphi(||Sv - Tv||) + \lambda||Sv - Sv^*|| \\ &\leq \lambda||Sv - Sv^*|| \\ &= \lambda||u - u^*||. \end{aligned}$$

This implies that $u = u^*$ as $\lambda \in [0, 1)$. Again, by the weak compatibility condition of S, T, from $Tu = TSv = TTv$, we obtain Tu as a point of coincidence of S and T. By the uniqueness of the point of coincidence, we have $u = Tu$. Consequently, $Su = u = Tu$; that is, S and T have a unique common fixed point, at which our Jungck–AI iterative procedure (4) converges. □

We provide the following theorem to demonstrate our iterative process (4) is stable.

Theorem 2. *Let A be a Banach space, and $S, T : B \longrightarrow A$ be two non-self mappings that satisfy the general contractive condition, defined on a non-empty subset B such that $T(B) \subseteq S(B)$ and $S(B)$ is complete in A. Then, the Jungck–AI iteration procedure $\{Su_n\}$ defined in (4) is $(S, T)^-$stable if $\{a_n\}$ is bounded away from 0.*

Proof. Suppose the iteration procedure $\{Su_n\}$ defined in (4) is given by $Su_{n+1} = F(u_n, T)$, for some function F and converges to a point of coincidence $Sv = Tv = u$, for some $v \in B$.

Now, let the sequence $\{Sz_n\}$ be arbitrary; then,

$$||Sz_{n+1} - u|| \leq ||Sz_{n+1} - F(z_n, T)|| + ||F(z_n, T) - u||,$$

where

$$\begin{cases} F(z_n, T) = Tv_n \\ Sv_n = Tw_n \\ Sw_n = Tx_n \\ Sx_n = a_nTz_n + (1 - a_n)Sz_n, \ n \in \mathbb{N}. \end{cases}$$

Proceeding similar to Theorem 1, we have

$$||Sz_{n+1} - u|| \leq ||Sz_{n+1} - F(z_n, T)|| + \lambda^3(1 - a_n(1 - \lambda))||Sz_n - u||.$$

On setting $\delta_n = ||Sz_{n+1} - F(z_n, T)||$, $\eta_n = a_n(1 - \lambda)$ and $\gamma_n = ||Sz_n - u||$, we see, if $\lim_{n\to+\infty} ||Sz_{n+1} - F(z_n, T)|| = 0$ and as $\{a_n\}$ is a bounded away sequence from 0, i.e., a non-negative sequence, then, by Lemma 1, $\lim_{n\to+\infty} \gamma_n = 0$, i.e., $\lim_{n\to+\infty} ||Sz_n - u|| = 0$, i.e., $\lim_{n\to+\infty} Sz_n = u$.

Conversely, let $\lim_{n\to+\infty} Sz_n = u$, i.e., $\lim_{n\to+\infty} ||Sz_n - u|| = 0$ and $\lim_{n\to+\infty} ||Sz_{n+1} - u|| = 0$. Then, $||Sz_{n+1} - F(z_n, T)||$

$$\begin{aligned} &\leq ||Sz_{n+1} - u|| + ||F(z_n, T) - u|| \\ &\leq ||Sz_{n+1} - u|| + \lambda^3(1 - a_n(1 - \lambda))||Sz_n - u||. \end{aligned}$$

which implies $\lim_{n\to+\infty} ||Sz_{n+1} - F(z_n, T)|| = 0$. That is, the iteration procedure $\{Su_n\}$ defined in (4) is stable with respect to S, T or (S, T)-stable. □

Remark 1. *In the following numerical calculations for the iterative procedure* $\{Su_n\}$ *defined in (4), we utilize the sequence outlined below:*

- *Start with an initial point* $u_1 \in B$.
- *Compute a value* $Sv_2 = F(u_1, T)$, *which is approximately equal to* Su_2 ($Sv_2 \approx Su_2$) *rather than an exact representation of* Su_2 *due to computational limitations.*
- *Next, compute* $Sv_3 = F(u_2, T) \approx Su_3$ *using the next term in the sequence,* $Su_3 = F(u_2, T)$.

Ultimately, we obtain a numerically approximated sequence $\{Sv_n\}$ *corresponding to the conceptual sequence* $\{Su_n\}$. *At each iteration, if* Sv_n *remains sufficiently close to* Su_n *and continues to converge to the common fixed point u of S and T, the fixed point reached by the iterations will be considered numerically stable or stable.*

We now demonstrate numerically that our Jungck–AI iterative method (4) converges faster than the three previous iteration methods introduced by Chugh et al. [40], Hussain et al. [42], and Guran et al. [43].

Example 1. *Let* $S, T : [1, 3] \longrightarrow [1, 27]$ *be two mappings defined as* $Su = u^3$, $Tu = 3u + 2$. *Then, from Figure 1 below and for* $\lambda = \frac{3}{4}$, $\varphi(t) = 2t$, S, T *satisfies the general contractive condition.*

Now, for sequences $\left\{a_n = \frac{1}{n^2}\right\}, \left\{b_n = \frac{1}{2}\right\}, \left\{c_n = \frac{1}{n+1}\right\} \subseteq (0, 1)$ *and the initial guess* $u_1 = 1$, *Table 1 and Figure 2 below represent the iterations of Chugh et al. [40], Hussain et al. [42] and Guran et al. [43] and our Jungck–AI iteration (4) converging to the point of coincidence 8 of* S, T *with the stop criterion* $||u_n - u|| < 10^{-5}$.

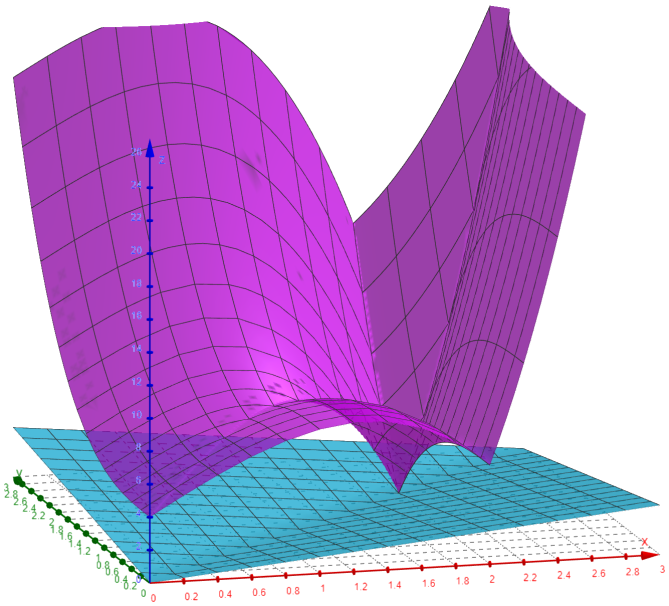

Figure 1. The surface above illustrates the right-hand-side term, while the surface below represents the left-hand-side term of the inequality in the general contractive condition.

Remark 2. *It is important to note that in Example 1, the mappings S and T are not weakly compatible. As a result, the iteration converges to a point of coincidence rather than a common fixed point.*

In the following example, we not only showcase the faster convergence of our iteration to a unique common fixed point but also explore and compare the effect of different parameters on the initial points.

Example 2. *In the Banach space* $([3,+\infty), d_u)$, *let* $S, T : [3,+\infty) \longrightarrow [3,+\infty)$ *be two mappings described as* $Su = \frac{u^4}{16} - 75$, $Tu = u^2 - 6u + 6$, *where* d_u *is the usual metric of* $\mathbb{R}$. *Then for* $\lambda = \frac{1}{5}$ *and* $\varphi(t) = 3t$, *Figure 3 below shows that* S, T *satisfies the general contractive condition.*

Now, for sequences $\left\{a_n = \frac{1+n}{2+n^2}\right\}, \left\{b_n = \frac{1}{1+n}\right\}, \left\{c_n = \frac{i}{2n+3}\right\} \subseteq (0,1)$, *the initial value* $u_1 = 4$, *and the stop criterion* $||u_n - u|| < 10^{-5}$, *Table 2 and Figure 4 below show the iterations of Chugh et al. [40], Hussain et al. [42], and Guran et al. [43] and our Jungck–AI iteration (4) converging to a unique common fixed point* $S6 = T6 = 6$.

Table 1. Comparison of iterations.

Steps	Jungck–SP (1)	Jungck–CR (2)	Jungck–DK (3)	Jungck–AI (4)
0	1	1	1	1
1	7.0121	7.3474	6.7878	7.9430
2	7.6188	7.8809	7.7186	7.9993
3	7.8218	7.9751	7.9325	8
4	7.9096	7.9945	7.9836	8
5	7.9520	7.9988	7.9960	8
6	7.9738	7.9997	7.9990	8
7	7.9854	7.9999	7.9998	8
8	7.9917	8	7.9999	8
9	7.9953	8	8	8
⋮	⋮	⋮	⋮	⋮
17	7.9999	8	8	8
18	8	8	8	8

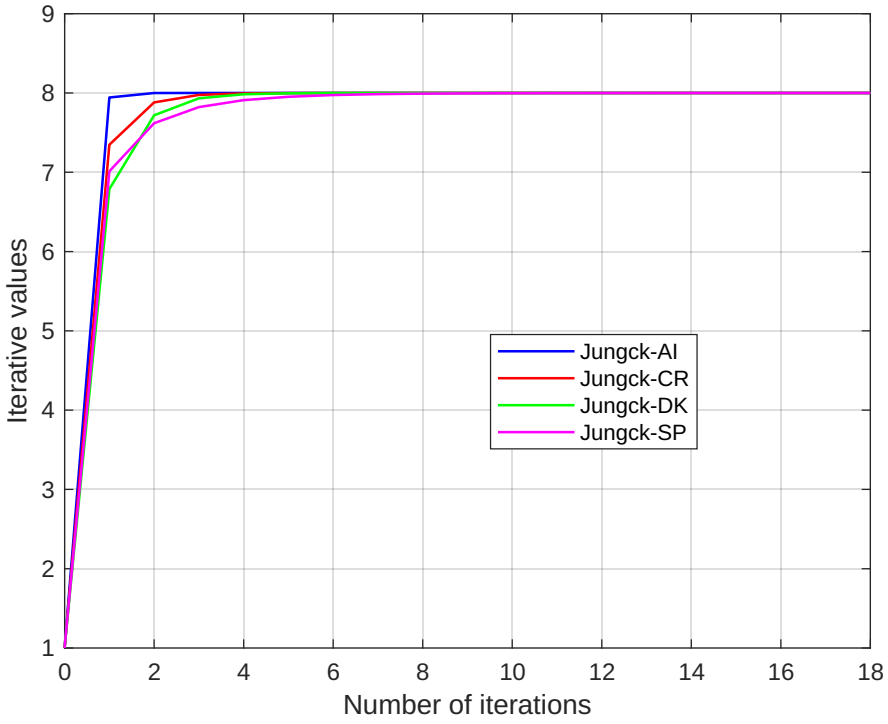

Figure 2. Convergence of iterations.

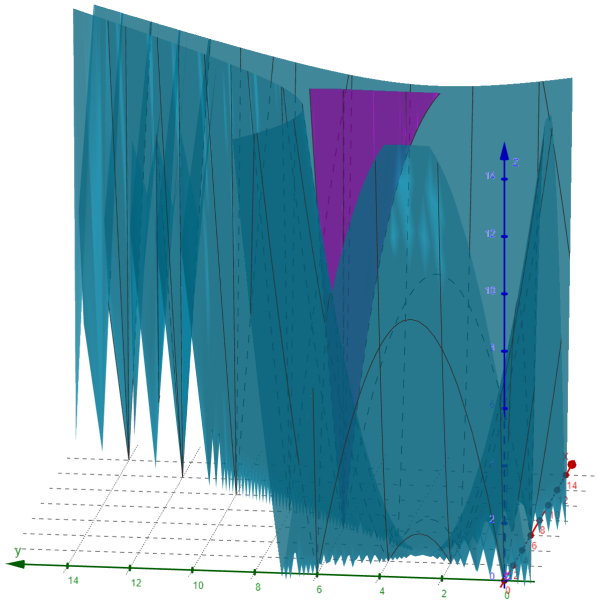

Figure 3. The surface above illustrates the right-hand-side term, while the surface below represents the left-hand-side term of the inequality in the general contractive condition.

Table 2. Comparison of iterations.

Steps	Jungck–SP (1)	Jungck–CR (2)	Jungck–DK (3)	Jungck–AI (4)
0	9	9	9	9
1	63.705	16.100	25.194	6.1473
2	22.654	6.5624	7.7380	6.0001
3	12.152	6.0391	6.1753	6
4	8.5756	6.0031	6.0184	6
5	7.1583	6.0003	6.0020	6
6	6.5449	6	6.0002	6
7	6.2642	6	6	6
8	6.1309	6	6	6
9	6.0659	6	6	6
⋮	⋮	⋮	⋮	⋮
20	6.0001	6	6	6
21	6	6	6	6

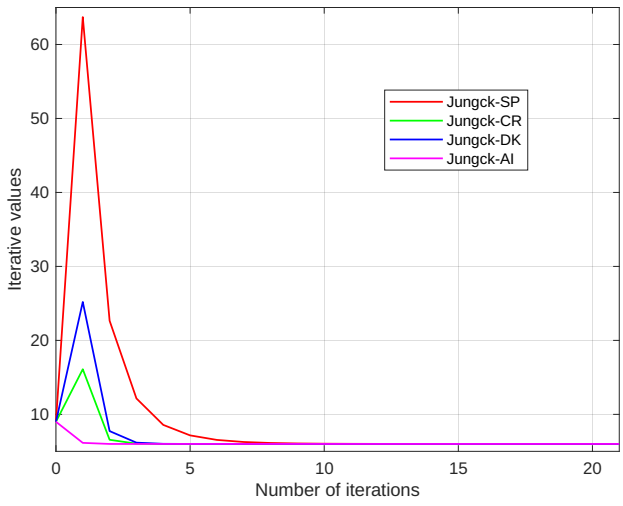

Figure 4. Convergence of iterations.

Table 3 below shows the effect of the initial value and parameters in comparison to the other methods. Numerically, we observe that the sequence generated by (4) converges more rapidly to a unique common fixed point of S and T when compared to the other iterations given by (1)–(3).

Table 3. Impact of parameters on the initial points for different iteration procedures.

Initial Points	**0**	**5**	**11**	**265**	**688**	**1721**	**3264**
$a_n = \frac{4n}{n^2+5}, b_n = \frac{n}{2n+7}, c_n = \frac{n+3}{(7n+1)^3}$							
Jungck–SP (1)	14	13	17	33	39	44	47
Jungck–CR (2)	5	6	7	9	10	10	10
Jungck–DK (3)	6	6	7	9	9	10	10
Jungck–AI (4)	2	2	3	3	3	3	3
$a_n = \frac{n+2}{4n+1}, b_n = \frac{3n}{(3n+8)^2}, c_n = \frac{1}{n^2+1}$							
Jungck–SP (1)	42	40	50	93	106	119	127
Jungck–CR (2)	5	7	8	10	10	10	10
Jungck–DK (3)	7	7	8	10	10	10	10
Jungck–AI (4)	2	2	3	3	4	4	4
$a_n = \frac{5}{7}, b_n = \frac{3}{4}, c_n = \frac{89}{90}$							
Jungck–SP (1)	3	4	4	6	7	7	8
Jungck–CR (2)	3	4	4	6	6	6	6
Jungck–DK (3)	5	5	6	8	8	8	8
Jungck–AI (4)	2	2	3	3	3	4	4
$a_n = \frac{13}{14}, b_n = \frac{n+1}{n+4}, c_n = \frac{n+2}{n+9}$							
Jungck–SP (1)	5	5	6	9	10	10	11
Jungck–CR (2)	4	4	4	6	6	6	6
Jungck–DK (3)	5	5	6	8	8	8	8
Jungck–AI (4)	2	2	2	3	3	3	3

4. Generation of Fractals as Julia and Mandelbrot Sets

The general escape criterion of the Jungck–AI orbit with an s-convex combination connected to transcendental sine functions in the complex plane is examined in this section. Using MATHEMATICA 12.3, we generate non-traditional chaotic fractals, specifically Julia and Mandelbrot sets, within the Jungck–AI orbit, incorporating s-convexity. The range of the area extends from $[-0.3, 0.3] \times [-0.3, 0.3]$ to $[-7, 7] \times [-7, 7]$. The computations were conducted on a system with an 11th Gen Intel(R) Core(TM) i3-1115G4 (Realme Book, DLF Cyber City, Gurgaon, India) processor operating at 3.00 GHz, equipped with 8 GB of DDR3 RAM, running Microsoft Windows 11 Home Single Language (64-bit), Version 24H2, OS build 26063.1, and Feature Experience Pack 1000.26063.1.0.

In the Jungck–AI iteration, we now substitute the concept of s-convex combination to obtain the Jungck–AI orbit with s-convexity.

Definition 7. *In the complex plane $\mathbb{C}$, let $S, T : \mathbb{C} \longrightarrow \mathbb{C}$ be two self-mappings. Then, the Jungck–AI orbit with s-convexity is described as*

$$\begin{cases} Su_{n+1} = Tv_n \\ Sv_n = Tw_n \\ Sw_n = Tx_n \\ Sx_n = a^s Tu_n + (1-a)^s Su_n, \ \forall n \in \mathbb{N} \cup \{0\}, \end{cases} \tag{5}$$

for random choice $u_0 \in \mathbb{C}$, where $a, s \in (0, 1]$.

Remark 3. *The reason for selecting the Jungck–AI iteration with s-convexity in generating Julia and Mandelbrot fractals lies in the property that all iterations—Chugh et al. [40], Hussain et al. [42], Guran et al. [43] and all Jungck-type iterative procedures (including Singh et al. [45], Olatinwo et al. [41], Kang et al. [11], Antal et al. [37], and many more)—converge to a coincidence point. But the Jungck–AI iteration with s-convexity demonstrates faster convergence compared to Chugh et al. [40], Hussain et al. [42], Guran et al. [43] and all Jungck-type iterative procedures (including Singh et al. [45], Olatinwo et al. [41], Kang et al. [11], Antal et al. [37], and many more).*

Since the Jungck–AI iteration involves two mappings, the number of mappings employed in the iteration should be considered when substituting the Jungck–AI orbit for other well-known orbits. We employ a certain process to deal with this.

Here, we consider transcendental sine functions of the type $\sin(u^m) - \alpha u + \beta$, for $u, \alpha, \beta \in \mathbb{C}, m \geq 2$, which can be written as $Tu - Su$, where $Su = \alpha u$ and $Tu = \sin(u^m) + \beta$. Apart from the reconstruction, where S is one-to-one, it is also necessary to create a new escape criterion and the iteration procedure (5).

For the function $\sin(u^m)$, we know that

$$|\sin(u^m)| = \left| u^m - \frac{u^{3m}}{3!} + \frac{u^{5m}}{5!} - \cdots \right| = |u^m| \left| 1 - \frac{u^{2m}}{3!} + \frac{u^{4m}}{5!} - \cdots \right|,$$

for all $u \in \mathbb{C}$.

Now consider $\mathbb{A}$ as the set of all $u \in \mathbb{C}$ so that $\sin(u^m) \neq 0$. Then, we can write

$$\frac{|\sin(u^m)|}{|u^m|} = \left| 1 - \frac{u^{2m}}{3!} + \frac{u^{4m}}{5!} - \cdots \right|, \text{ for all } u \in \mathbb{A}.$$

For fixed $u \in \mathbb{A}$, let $\gamma_u = \min\left\{1, \frac{|\sin(u^m)|}{|u^m|}\right\}$, then $0 < |\gamma_u| \leq 1$ and $|\sin(u^m)| \geq |\gamma_u||u^m|$. Again, let $u_0 \in \mathbb{A}$ and $\mathbb{A}_{u_0} = \{u \in \mathbb{A} : |u| > |u_0|\}$; then, we can define a number $\gamma = \inf\{\gamma_u : u \in \mathbb{A}\}$ so that $0 < |\gamma| \leq 1$ and $|\sin(u^m)| \geq |\gamma||u^m|$, for all $u \in \mathbb{A}_{u_0}$.

For the defined orbit, the following is an escape criterion.

Theorem 3. *The Jungck–AI orbit $\{u_n\}$ with s-convexity defined in (5) is so that $|u_n| \to +\infty$ whenever $n \to +\infty$, if*

$$|u| \geq |\beta| \geq \left(\frac{2|\alpha|}{|\gamma_1|}\right)^{\frac{1}{m-1}}, |u| \geq |\beta| \geq \left(\frac{2|\alpha|}{|\gamma_2|}\right)^{\frac{1}{m-1}},$$

$$|u| \geq |\beta| \geq \left(\frac{2|\alpha|}{|\gamma_3|}\right)^{\frac{1}{m-1}} \text{ and } |u| \geq |\beta| \geq \left(\frac{2(|\alpha|+1)}{as|\gamma_4|}\right)^{\frac{1}{m-1}}.$$

Proof. For $n = 0$, let $u_0 = u$. Then, from the Jungck–AI iteration procedure with s-convexity, we have

$$\begin{aligned} |S x_0| &= |a^s Tu_0 + (1-a)^s Su_0| \\ &= |a^s Tu + (1-a)^s Su| \\ &= |a^s[\sin(u^m) + \beta] + (1-a)^s \alpha u| \\ &\geq |a^s|[|\sin(u^m)| - |\beta|] - |(1-a)^s \alpha u|. \end{aligned}$$

Now, there exists $\gamma_4 \in \mathbb{C}$ with $|\gamma_4| \in (0,1]$ so that $|\sin(u^m)| \geq |\gamma_4||u^m|$, for all $u \in \mathbb{C}$ but for which $|\gamma_4| = 0$. Also, $a, s \in (0,1]$ implies $a^s \geq as$, and from the binomial expansion of $(1-a)^s$, we have $(1-a)^s \leq 1 - as < 1$. Hence, utilizing $|u| \geq |\beta|$, we obtain

$$\begin{aligned} |\alpha||x_0| &\geq as[|\gamma_4||u^m| - |u|] - |\alpha||u| \\ &\geq as|\gamma_4||u^m| - |u| - |\alpha||u|, \text{ since } as < 1 \\ &= |u|(|\alpha|+1)\Big(\tfrac{as|\gamma_4||u^{m-1}|}{|\alpha|+1} - 1\Big). \end{aligned}$$

Since $|\alpha| + 1 > \alpha$ and $|u| \geq \left(\frac{2(|\alpha|+1)}{as|\gamma_4|}\right)^{\frac{1}{m-1}}$, we have $|x_0| \geq |u| \geq |\beta|$.
This brings us to the next iteration of the Jungck–AI procedure for $x_0 = x$:

$$\begin{aligned} |Sw_0| &= |Tx_0| \\ &= |Tx| \\ &= |\sin(x^m) + \beta| \\ &\geq |\sin(x^m)| - |\beta|. \end{aligned}$$

Now, there exists $\gamma_3 \in \mathbb{C}$ with $|\gamma_3| \in (0,1]$ so that $|\sin(x^m)| \geq |\gamma_3||x^m|$, for all $x \in \mathbb{C}$ but for which $|\gamma_3| = 0$. Hence, utilizing $|x| \geq |u| \geq |\beta|$, we obtain

$$\begin{aligned} |\alpha||w_0| &\geq |\gamma_3||x^m| - |x| \\ &= |x|\big(|\gamma_3||x^{m-1}| - 1\big) \\ \Rightarrow |w_0| &\geq |x|\Big(\tfrac{|\gamma_3||x^{m-1}|}{|\alpha|} - 1\Big). \end{aligned}$$

Since $|x| \geq \left(\frac{2|\alpha|}{|\gamma_3|}\right)^{\frac{1}{m-1}}$, we have $|w_0| \geq |x| \geq |u| \geq |\beta|$.
This brings us to the next iteration of the Jungck–AI procedure for $w_0 = w$:

$$\begin{aligned} |Sv_0| &= |Tw_0| \\ &= |Tw| \\ &= |\sin(w^m) + \beta| \\ &\geq |\sin(w^m)| - |\beta|. \end{aligned}$$

Now, there exists $\gamma_2 \in \mathbb{C}$ with $|\gamma_2| \in (0,1]$ so that $|\sin(w^m)| \geq |\gamma_2||w^m|$, for all $w \in \mathbb{C}$ but for which $|\gamma_2| = 0$. Hence, utilizing $|w| \geq |x| \geq |u| \geq |\beta|$, we obtain

$$\begin{aligned} |\alpha||v_0| &\geq |\gamma_2||w^m| - |w| \\ &= |w|\big(|\gamma_3||w^{m-1}| - 1\big) \\ \Rightarrow |v_0| &\geq |w|\Big(\tfrac{|\gamma_3||w^{m-1}|}{|\alpha|} - 1\Big). \end{aligned}$$

Since $|w| \geq \left(\frac{2|\alpha|}{|\gamma_2|}\right)^{\frac{1}{m-1}}$, we have $|v_0| \geq |w| \geq |x| \geq |u| \geq |\beta|$.
This brings us to the next iteration of the Jungck–AI procedure for $v_0 = v$

$$\begin{aligned} |Su_1| &= |Tv_0| \\ &= |Tv| \\ &= |\sin(v^m) + \beta| \\ &\geq |\sin(v^m)| - |\beta|. \end{aligned}$$

Now, there exists $\gamma_1 \in \mathbb{C}$ with $|\gamma_1| \in (0,1]$ so that $|\cos(v^m)| \geq |\gamma_1||v^m|$, for all $v \in \mathbb{C}$ but for which $|\gamma_1| = 0$. Hence, utilizing $|v| \geq |w| \geq |x| \geq |u| \geq |\beta|$, we obtain

$$\begin{aligned} |\alpha||u_1| &\geq |\gamma_1||v^m| - |v| \\ &= |v|\big(|\gamma_1||v^{m-1}| - 1\big) \\ \Rightarrow |u_1| &\geq |u|\Big(\tfrac{|\gamma_1||v^{m-1}|}{\alpha} - 1\Big). \end{aligned}$$

Consequently, for $n = 1$, we have

$$\begin{aligned} |u_2| &\geq |u_1|\Big(\tfrac{|\gamma_1||v^{m-1}|}{\alpha} - 1\Big) \\ &\geq |u|\Big(\tfrac{|\gamma_1||v^{m-1}|}{\alpha} - 1\Big)^2. \end{aligned}$$

Continuing the iteration, we have

$$\begin{aligned} |u_3| &\geq |u|\Big(\tfrac{|\gamma_1||v^{m-1}|}{\alpha} - 1\Big)^3, \\ |u_4| &\geq |u|\Big(\tfrac{|\gamma_1||v^{m-1}|}{\alpha} - 1\Big)^4, \\ &\vdots \\ |u_n| &\geq |u|\Big(\tfrac{|\gamma_1||v^{m-1}|}{\alpha} - 1\Big)^n. \end{aligned}$$

Since $|u| \geq \left(\frac{2|\alpha|}{|\gamma_1|}\right)^{\frac{1}{m-1}}$, we have $|u_n| \to +\infty$ as $n \to +\infty$. □

Now we present subsequent corollaries that offer exploration methods for Julia and Mandelbrot sets.

Corollary 1. *The Jungck–AI orbit $\{u_n\}$ with s-convexity defined in (5) escapes to infinity if*

$$|u| \geq |\beta| \geq \max\left\{\left(\frac{2|\alpha|}{|\gamma_1|}\right)^{\frac{1}{m-1}}, \left(\frac{2|\alpha|}{|\gamma_2|}\right)^{\frac{1}{m-1}}, \left(\frac{2|\alpha|}{|\gamma_3|}\right)^{\frac{1}{m-1}}, \left(\frac{2(|\alpha|+1)}{as|\gamma_4|}\right)^{\frac{1}{m-1}}\right\}.$$

Corollary 2. *The Jungck–AI orbit $\{u_n\}$ with s-convexity defined in (5) escapes to infinity if*

$$|u| \geq \max\left\{|\beta|, \left(\frac{2|\alpha|}{|\gamma_1|}\right)^{\frac{1}{m-1}}, \left(\frac{2|\alpha|}{|\gamma_2|}\right)^{\frac{1}{m-1}}, \left(\frac{2|\alpha|}{|\gamma_3|}\right)^{\frac{1}{m-1}}, \left(\frac{2(|\alpha|+1)}{as|\gamma_4|}\right)^{\frac{1}{m-1}}\right\}.$$

While fractal geometry and complex numbers are foundational to both Julia sets and Mandelbrot sets, these are distinct mathematical constructs with key differences, as illustrated by the algorithms in Tables 4 and 5. For the Julia set algorithm, typically presented in Table 4, various initial values of u_0 are used with a fixed parameter β to observe which points remain bounded and which diverge to infinity. In contrast, the Mandelbrot set algorithm in Table 5 consistently starts with $u_0 = 0$ for each iteration.

Table 4. Algorithm for the generation of fractals as Julia sets.

1.	Setup:
(i)	Define the functions $Su = \alpha u$ and $Tu = \sin(u^m) + \beta$.
(ii)	Consider a complex number $\beta = p + iq$
(iii)	Set the variables $\alpha, a, \gamma_1, \gamma_2, , \gamma_3, \gamma_4, m, n, s, p, q$ to their initial values
(iv)	Take into account the initial iteration $u_0 = x + iy$
2.	Iterate:
	$Su_{n+1} = Tv_n$ $Sv_n = Tw_n$ $Sw_n = Tx_n$ $Sx_n = a^s Tu_n + (1-a)^s Su_n$
3.	Stop:
	$\|u\| \geq \max\left\{ \|\beta\|, \left(\frac{2\|\alpha\|}{\|\gamma_1\|}\right)^{\frac{1}{m-1}}, \left(\frac{2\|\alpha\|}{\|\gamma_2\|}\right)^{\frac{1}{m-1}}, \left(\frac{2\|\alpha\|}{\|\gamma_3\|}\right)^{\frac{1}{m-1}}, \left(\frac{2(\|\alpha\|+1)}{as\|\gamma_4\|}\right)^{\frac{1}{m-1}} \right\}$
4.	Count:
	The number of attempts made to escape.
5.	Colour:
	In accordance with the number of escape repetitions required.

Table 5. Algorithm for the generation of fractals as Mandelbrot sets.

1.	Setup:
(i)	Define the functions $Su = \alpha u$ and $Tu = \sin(u^m) + \beta$.
(ii)	Consider a complex number $\beta = x + iy$
(iii)	Set the variables $\alpha, a, \gamma_1, \gamma_2, , \gamma_3, \gamma_4, m, n, s$ to their initial values
(iv)	Take into account $u = \beta$
2.	Iterate:
	$Su_{n+1} = Tv_n$ $Sv_n = Tw_n$ $Sw_n = Tx_n$ $Sx_n = a^s Tu_n + (1-a)^s Su_n$
3.	Stop:
	$\|u\| \geq \max\left\{ \|\beta\|, \left(\frac{2\|\alpha\|}{\|\gamma_1\|}\right)^{\frac{1}{m-1}}, \left(\frac{2\|\alpha\|}{\|\gamma_2\|}\right)^{\frac{1}{m-1}}, \left(\frac{2\|\alpha\|}{\|\gamma_3\|}\right)^{\frac{1}{m-1}}, \left(\frac{2(\|\alpha\|+1)}{as\|\gamma_4\|}\right)^{\frac{1}{m-1}} \right\}$
4.	Count:
	The number of attempts made to escape.
5.	Colour:
	In accordance with the number of escape repetitions required.

4.1. Fractals as Julia Sets

This subsection demonstrates the behavior changes in Julia set fractals generated by the transcendental sine function within the Jungck–AI orbit, incorporating s-convexity. Notably, even slight adjustments to any parameter lead to substantial changes in the fractals' structure. Therefore, we systematically vary almost every parameter to produce fractals for our orbit, as illustrated in the images below.

The primary fractals created by adjusting the parameter m (as detailed in Table 6), while keeping other parameters constant, are shown in Figure 5. As m increases, the number of chaotic attractors in the fractals grows, and the fractals become increasingly circular.

Each Julia set contains $2m$ spokes. An interesting color shift is observed, with a grey tone at $m = 3$ and a yellow tone at $m = 7$, forming a visually appealing pattern. Additionally, the Julia fractal shape becomes progressively circular as m increases.

Table 6. Changes in parameter m for generating fractals as a Julia set.

	m	α	β	a	s	γ_1	γ_2	γ_3	γ_4
(i)	2	-2	$-1.4i$	0.936	0.928	0.056	0.012	0.003	0.006
(ii)	3	-2	$-1.4i$	0.936	0.928	0.056	0.012	0.003	0.006
(iii)	4	-2	$-1.4i$	0.936	0.928	0.056	0.012	0.003	0.006
(iv)	5	-2	$-1.4i$	0.936	0.928	0.056	0.012	0.003	0.006
(v)	6	-2	$-1.4i$	0.936	0.928	0.056	0.012	0.003	0.006
(vi)	7	-2	$-1.4i$	0.936	0.928	0.056	0.012	0.003	0.006

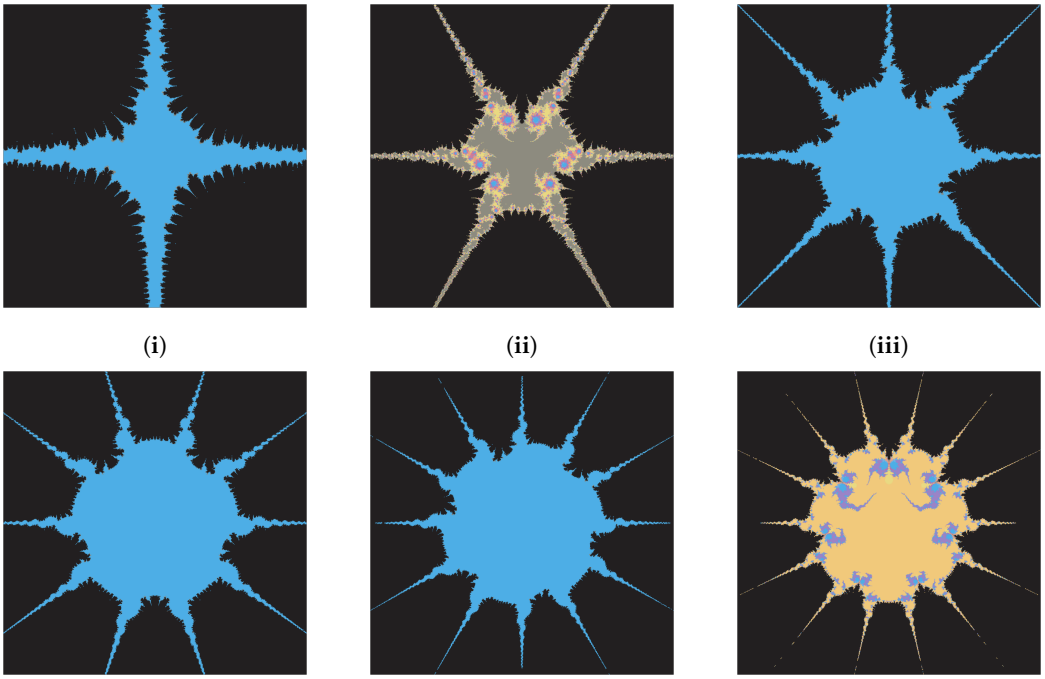

Figure 5. (**i–vi**) Effect of m on fractals as a Julia set.

Parameter α adds visual appeal to the fractals. A segment of the Julia set begins to separate as α changes from -1 to 0.8 (Figure 6i–iv). Distinct purple chaotic fractals emerge when the parameter α has a negative complex component (Table 7), as shown in Figure 6ii–v. Higher modulus values of α cause the fractal to distort.

Table 7. Changes in parameter α for generating fractals as a Julia set.

	m	α	β	a	s	γ_1	γ_2	γ_3	γ_4
(i)	4	-1	$-0.6 - 0.01i$	0.736	0.928	0.034	0.021	0.002	0.001
(ii)	4	$-0.4 - 0.7i$	$-0.6 - 0.01i$	0.736	0.928	0.034	0.021	0.002	0.001
(iii)	4	$1.1i$	$-0.6 - 0.01i$	0.736	0.928	0.034	0.021	0.002	0.001
(iv)	4	0.8	$-0.6 - 0.01i$	0.736	0.928	0.034	0.021	0.002	0.001
(v)	4	$0.7 + 0.3i$	$-0.6 - 0.01i$	0.736	0.928	0.034	0.021	0.002	0.001
(vi)	4	$0.6 - 0.5i$	$-0.6 - 0.01i$	0.736	0.928	0.034	0.021	0.002	0.001

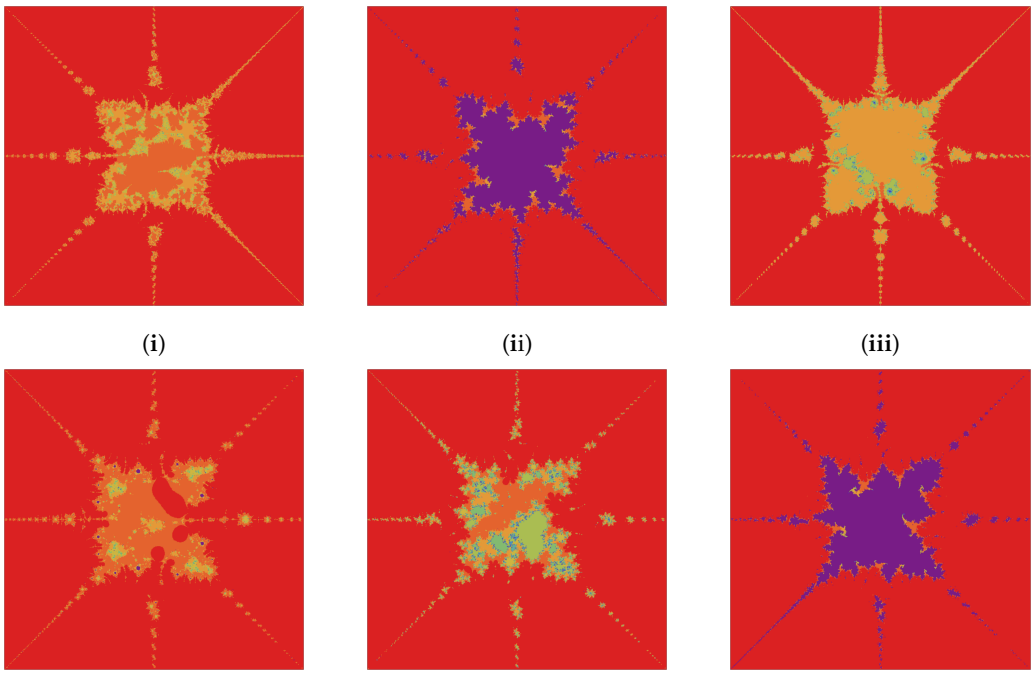

Figure 6. (**i–vi**) Effect of α on fractals as Julia sets.

Variations in color and form appear in Figure 7 for different values of β (Table 8), showing a resemblance to Rangoli patterns.

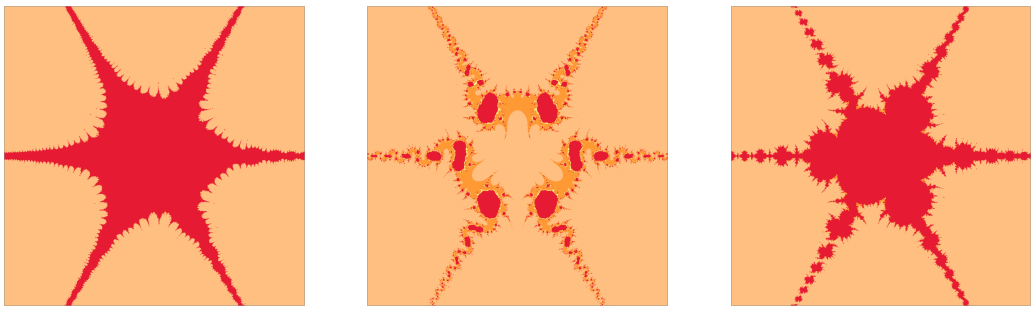

Figure 7. (**i–iii**) Effect of β on fractals as Julia sets.

Table 8. Changes in parameter β for generating fractals as Julia sets.

	m	α	β	a	s	γ_1	γ_2	γ_3	γ_4
(i)	3	-2	$-0.542 + 0.245i$	0.963	0.828	0.056	0.012	0.003	0.006
(ii)	3	-2	$2i$	0.963	0.828	0.056	0.012	0.003	0.006
(iii)	3	-2	$1 - i$	0.963	0.828	0.056	0.012	0.003	0.006

Changes in the basic shape occur as the convexity parameter increases, though colors remain the same. Larger values enhance the Julia set's aesthetic and make it suitable for textile design. With increasing values of the convex parameter s (Table 9), Figure 8 shows an increase in symmetrical chaotic forms within the fractals.

Table 9. Changes in parameter s for generating fractals as Julia sets.

	m	α	β	a	s	γ_1	γ_2	γ_3	γ_4
(i)	4	$1-1.3i$	$-0.4+1.5i$	0.017	0.26	0.056	0.078	0.095	0.063
(ii)	4	$1-1.3i$	$-0.4+1.5i$	0.017	0.56	0.056	0.078	0.095	0.063
(iii)	4	$1-1.3i$	$-0.4+1.5i$	0.017	0.96	0.056	0.078	0.095	0.063

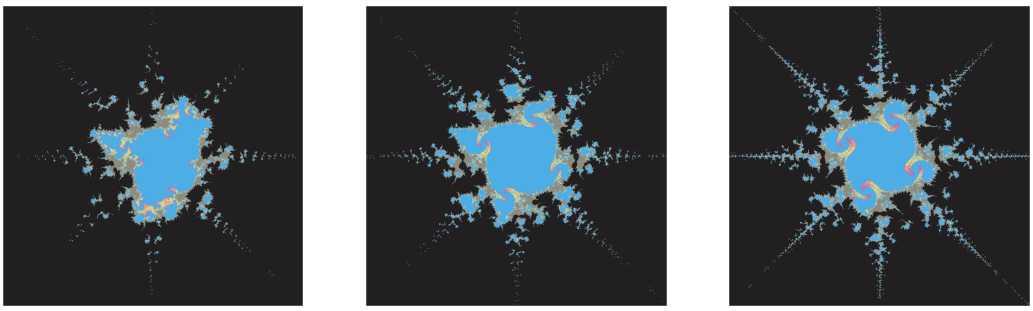

(i) **(ii)** **(iii)**

Figure 8. **(i–iii)** Effect of s on fractals as Julia sets.

The basic shape also transforms with higher values of the parameter a, while color saturation increases at higher a values. In Figure 9, more red appears in the center of the fractals as a increases (Table 10).

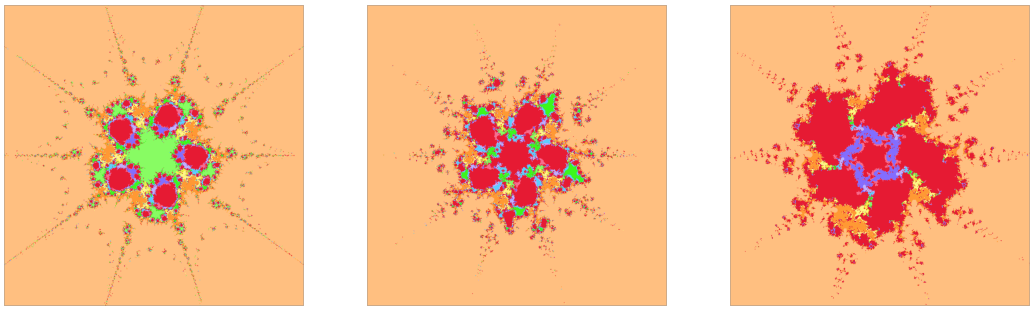

(i) **(ii)** **(iii)**

Figure 9. **(i–iii)** Effect of a on fractals as Julia sets.

Table 10. Changes in parameter a for generating fractals as Julia sets.

	m	α	β	a	s	γ_1	γ_2	γ_3	γ_4
(i)	5	$1.2i$	$-0.2+0.82i$	0.001	0.96	0.256	0.378	0.595	0.463
(ii)	5	$1.2i$	$-0.2+0.82i$	0.048	0.96	0.256	0.378	0.595	0.463
(iii)	5	$1.2i$	$-0.2+0.82i$	0.123	0.96	0.256	0.378	0.595	0.463

Only minimal changes occur in the fractals shown in Figure 10 as the parameters $\gamma_1, \gamma_2, \gamma_3$, and γ_4 vary (Table 11).

Table 11. Changes in parameters $\gamma_1, \gamma_2, \gamma_3, \gamma_4$ for generating fractals as Julia sets.

	m	α	β	a	s	γ_1	γ_2	γ_3	γ_4
(i)	2	-2.1	$1.7-1.6i$	0.001	0.99	0.004	0.002	0.001	0.003
(ii)	2	-2.1	$1.7-1.6i$	0.001	0.99	0.294	0.192	0.391	0.293
(iii)	2	-2.1	$1.7-1.6i$	0.001	0.99	0.94	0.92	0.91	0.93

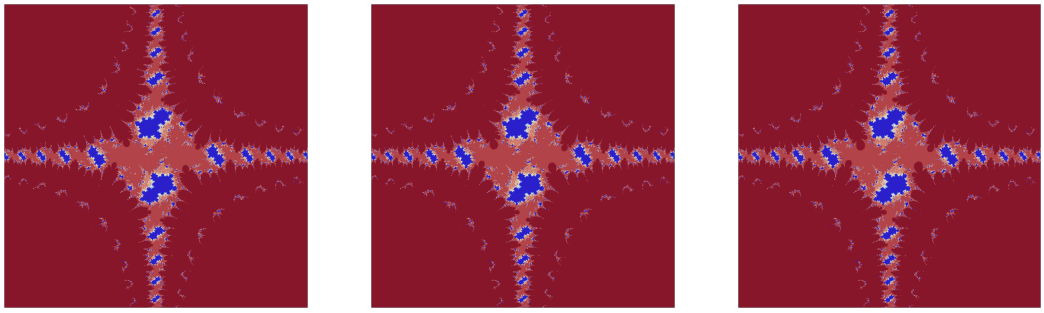

(i) (ii) (iii)

Figure 10. (**i–iii**) Effect of $\gamma_1, \gamma_2, \gamma_3, \gamma_4$ on fractals as Julia sets.

The fractals displayed in Figure 11 are derived from randomly selected parameters (Table 12).

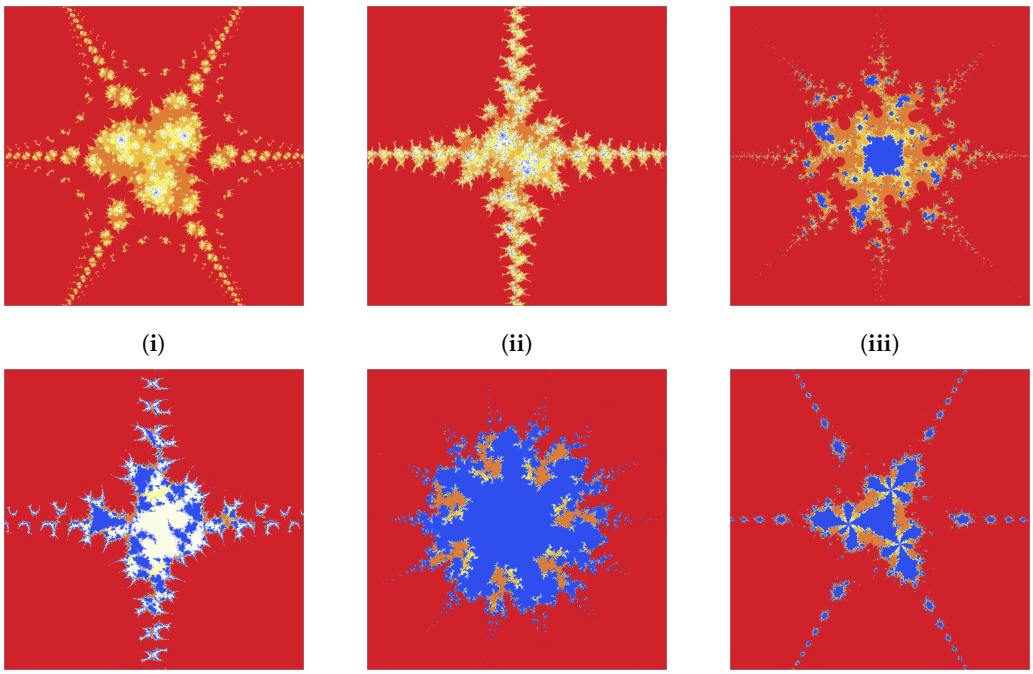

(i) (ii) (iii)

(iv) (v) (vi)

Figure 11. (**i–vi**) Effect of random choice of parameters on fractals as Julia sets.

Table 12. Random changes in parameters for generating fractals as Julia sets.

	m	α	β	a	s	γ_1	γ_2	γ_3	γ_4
(i)	3	-2.2	$1.8-1.5i$	0.002	0.89	0.034	0.042	0.074	0.98
(ii)	2	$-2.2-0.8i$	$-1.8+2i$	0.012	0.49	0.064	0.072	0.094	0.028
(iii)	4	$-2.4i$	$2.8i$	0.035	0.872	0.566	0.457	0.873	0.867
(iv)	2	-2.7	$1.3-1.8i$	0.007	0.086	0.435	0.568	0.657	0.874
(v)	7	$3.4i$	$-1+2.8i$	0.061	0.784	0.023	0.065	0.098	0.054
(vi)	3	$0.8+0.7i$	0.9	0.999	0.961	0.263	0.152	0.542	0.123

4.2. Fractals as Mandelbrot Sets

This section also explores behavior shifts in fractals as Mandelbrot sets generated by the transcendental sine function within the Jungck–AI orbit with s-convexity. Small parameter modifications cause significant changes in the fractals. Thus, we altered each parameter to generate the fractals in the images below.

Adjusting m (Table 13) while keeping other parameters fixed produces the fractals shown in Figure 12. As m increases, the number of chaotic attractors grows, and each Mandelbrot set has $2m$ major blue attractors.

Table 13. Parameters for generating fractals as Mandelbrot sets.

	m	α	a	s	γ_1	γ_2	γ_3	γ_4
(i)	2	2	0.076	0.036	0.035	0.068	0.057	0.056
(ii)	3	2	0.076	0.036	0.035	0.068	0.057	0.056
(iii)	4	2	0.076	0.036	0.035	0.068	0.057	0.056
(iv)	5	2	0.076	0.036	0.035	0.068	0.057	0.056
(v)	6	2	0.076	0.036	0.035	0.068	0.057	0.056
(vi)	7	2	0.076	0.036	0.035	0.068	0.057	0.056

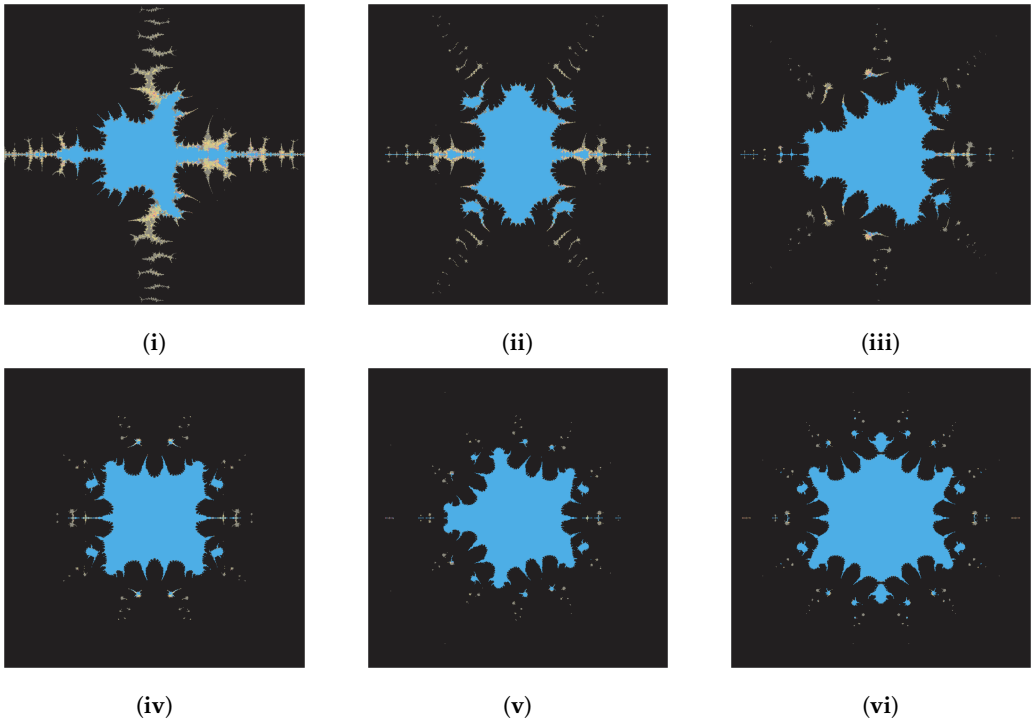

Figure 12. (**i**–**vi**) Effect of m on fractals as Mandelbrot sets.

Parameter α enhances the aesthetic quality of the fractals. Visually appealing fractals appear in Figure 13, while other parameters are kept constant (Table 14). Complex values of α emphasize the central region.

Table 14. Changes in parameter α for generating fractals as Mandelbrot sets.

	m	α	a	s	γ_1	γ_2	γ_3	γ_4
(i)	3	$2.5 + i$	0.001	0.704	0.867	0.897	0.567	0.765
(ii)	3	$6 - 1.5i$	0.001	0.704	0.867	0.897	0.567	0.765
(iii)	3	$-1 + i$	0.001	0.704	0.867	0.897	0.567	0.765
(iv)	3	-0.3	0.001	0.704	0.867	0.897	0.567	0.765
(v)	3	0.6	0.001	0.704	0.867	0.897	0.567	0.765
(vi)	3	$1.1i$	0.001	0.704	0.867	0.897	0.567	0.765

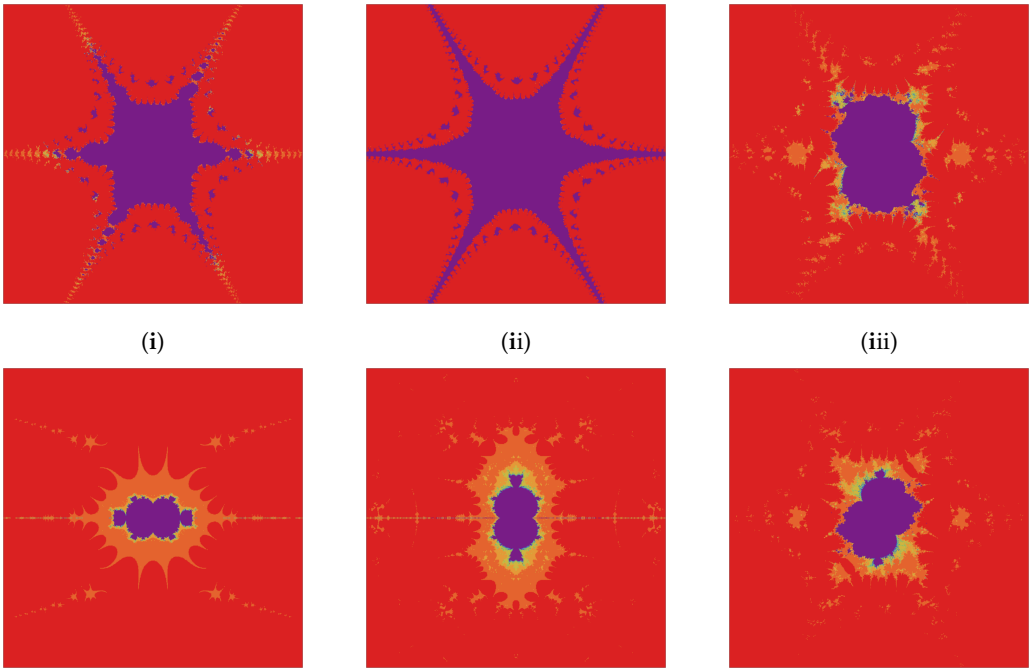

Figure 13. (**i**–**vi**) Effect of α on fractals as Mandelbrot sets.

Figure 14 (Table 15) demonstrates that small changes in the convex parameter s significantly affect the fractals. Lower s values brighten the Mandelbrot set's perimeter.

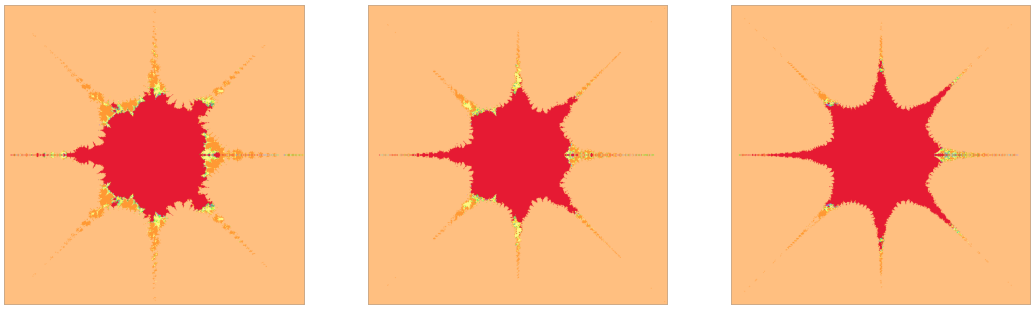

Figure 14. (**i**–**vi**) Effect of s on fractals as Mandelbrot set.

Table 15. Changes in parameter s for generating fractals as Mandelbrot sets.

	m	α	a	s	γ_1	γ_2	γ_3	γ_4
(i)	4	−2	0.534	0.054	0.078	0.075	0.065	0.057
(ii)	4	−2	0.534	0.454	0.078	0.075	0.065	0.057
(iii)	4	−2	0.534	0.954	0.078	0.075	0.065	0.057

The fractals in Figure 15 turn blue with increasing values of parameter a (Table 16), and the shape transforms as a increases.

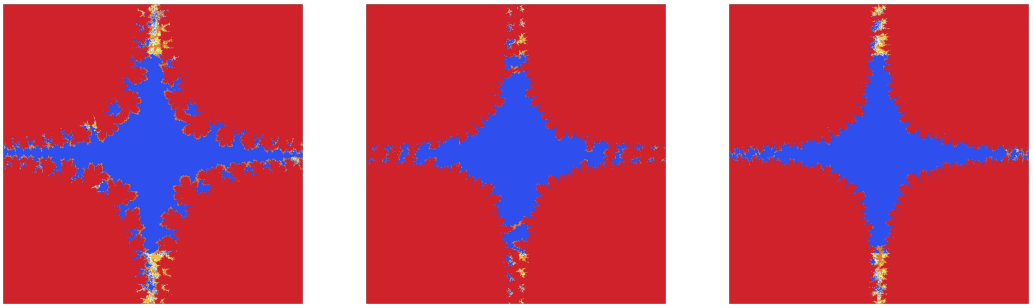

(i) (ii) (iii)

Figure 15. (**i**–**iii**) Effect of a on fractals as Mandelbrot sets.

Table 16. Changes in parameter a for generating fractals as Mandelbrot sets.

	m	α	a	s	γ_1	γ_2	γ_3	γ_4
(i)	2	$-3i$	0.034	0.999	0.021	0.013	0.043	0.023
(ii)	2	$-3i$	0.634	0.999	0.021	0.013	0.043	0.023
(iii)	2	$-3i$	0.934	0.999	0.021	0.013	0.043	0.023

As with Julia sets, Mandelbrot fractals show minimal variation with changes to parameters $\gamma_1, \gamma_2, \gamma_3, \gamma_4$.

Remark 4. *These generated fractals have broad applications in fabric design, such as in Batik, Kalamkari, Tie and Dye, and other textile prints (e.g., Figures 5, 8, 10, 12, 14 and 15). They revolutionize textile design by providing intricate patterns, streamlining processes to save time and resources, enabling scalable designs across different fabric types, and allowing digital previews to minimize waste. This promotes global collaboration, fosters creativity, cuts costs, supports sustainability, and boosts competitiveness in the textile industry.*

5. Conclusions

Our study presented a novel iterative approach, namely the Jungck–AI iteration procedure, for approximating unique common fixed points of general contractive mappings. We provided theorems to demonstrate the convergence and stability of this iteration process with examples and graphs. Additionally, we established that Jungck–AI(4) converges to the point of coincidence more quickly than Jungck–SP, Jungck–CR, Jungck–DK, and other similar methods. With s-convexity, and for the subsequent orbit, we generated fractals as Julia and Mandelbrot sets for the transcendental sine function $T_{\alpha,\beta}(u) = \sin(u^m) - \alpha u + \beta$, for $u, \alpha, \beta \in \mathbb{C}$ and $m \geq 2$. We provided a theorem to demonstrate the escape criterion for the sine function and the orbit with the convexity condition. Additionally, we explored the following impacts of the involved parameters on the color deviance, appearance, and dynamics of generated chaotic fractals.

- It is unexpected to observe that, given the same set of values, even little changes in one parameter have a significant influence on how the resulting fractal appears during the generation process. As a result, choosing the right parameters is crucial to obtaining the desired fractal pattern.
- In both Julia and Mandelbrot fractals, the number of outer spokes is twice the value of the parameter m.
- The majority of fractals exhibit symmetry about the initial line.
- In the case of both Julia and Mandelbrot fractals, a small change in the convex parameter s is highly effective.

- The number of colors is typically limited in almost all fractals, and there exists a hollow portion in each of them.
- We notice that when we enlarge the Mandelbrot set at its petal edges, we encounter the Julia set, indicating that every Mandelbrot set point contains a significant amount of Julia set image data.

Fractal geometry is widely recognized for its ability to depict the intricacy of many complex forms found in our environment. The chaotic behaviors of fractals, in reality, are able to depict surfaces and forms that conventional Euclidean geometry is unable to convey (Figures 16 and 17).

```
(*Program Source Used for Generating the Julia Sets*)

T[u_] := Sin[u^m] + β;
iter[x_, y_, lim_] := Block[{β, z, m, α, p, q, a, s, i, j, k, l, ct},
  β = p + q I; z = x + y I; m = 2; α = -2.7; p = 1.3; q = -1.8; a = 0.006;
  s = 0.086; i = 0.435; j = 0.568; k = 0.657; l = 0.874;ct = 0;
  While[
   (Abs[z] < Max[Abs[β], ((2 * Abs[α]) / (Abs[i])) ^ (1 / (m - 1)),
       ((2 * Abs[α]) / (Abs[j])) ^ (1 / (m - 1)),
       ((2 * Abs[α]) / (Abs[k])) ^ (1 / (m - 1)),
       (2 * (Abs[α] + 1) / (a * s * Abs[l])) ^ (1 / (m - 1))]) && (ct ≤ lim), ++ct;
   g = (((1 - a) ^ s) * α * z + (a^s) * T[z]) / α;
   w = T[g] / α;
   h = T[w] / α;
   v = T[h] / α;
   z = v;
  ];
  Return[ct];
 ]
DensityPlot[-iter[x, y, 10], {x, -5, 5}, {y, -5, 5}, PlotPoints → 200,
 ColorFunction → "TemperatureMap", PlotLegends → Automatic,
 FrameStyle → None, Frame → None]
```

Figure 16. The Figure shows a source code for generating Julia set.

```
(*Program Source Used for Generating the Mandelbrot Sets*)

T[u_] := Sin[u^m] + β;
iter[x_, y_, lim_] := Block[{β, z, m, α, a, s, i, j, k, l, ct},
  β = x + y I; z = β; m = 5; α = 1 + 2 I; a = 0.004; s = 0.009;
  i = 0.021; j = 0.013; k = 0.043; l = 0.023; ct = 0;
  While[
   (Abs[z] < Max[Abs[β], ((2 * Abs[α]) / (Abs[i])) ^ (1 / (m - 1)),
       ((2 * Abs[α]) / (Abs[j])) ^ (1 / (m - 1)),
       ((2 * Abs[α]) / (Abs[k])) ^ (1 / (m - 1)),
       (2 * (Abs[α] + 1) / (a * s * Abs[l])) ^ (1 / (m - 1))]) && (ct ≤ lim), ++ct;
   g = (((1 - a) ^ s) * α * z + (a^s) * T[z]) / α;
   w = T[g] / α;
   h = T[w] / α;
   v = T[h] / α;
   z = v;
  ];
  Return[ct];
 ]
DensityPlot[-iter[x, y, 10], {x, -6, 6}, {y, -6, 6}, PlotPoints → 200,
 ColorFunction → "ThermometerColors", PlotLegends → Automatic,
 FrameStyle → None, Frame → None]
```

Figure 17. The Figure shows a source code for generating Mandelbrot set.

Author Contributions: Conceptualization, N.S., K.H.A. and Y.R.; methodology, N.S., K.H.A. and Y.R.; validation, A.T., Y.R. and M.A.; formal analysis, N.S., Y.R. and A.T.; resources, M.A.; writing—original draft preparation, K.H.A. and N.S.; writing—review and editing, N.S. and A.R.; visualization, K.H.A., Y.R. and M.A.; funding acquisition, N.S. and M.A. All the authors discussed the results and contributed to the final manuscript. All authors have read and agreed to the published version of the manuscript.

Funding: This work was supported by the Deanship of Scientific Research, Vice Presidency for Graduate Studies and Scientific Research, King Faisal University, Saudi Arabia [KFU250082].

Institutional Review Board Statement: Not applicable.

Data Availability Statement: No new data were created or analyzed in this study. Data sharing is not applicable to this article.

Acknowledgments: The first author expresses gratitude to the University Grants Commission (UGC), New Delhi, India.

Conflicts of Interest: The authors declare that they have no conflicts of interest.

References

1. Alam, K.H.; Rohen, Y.; Tomar, A. (α,F)-Geraghty type generalized F-contractions on non-Archimedean fuzzy metric-unlike spaces. *Demonstr. Math.* **2024**, *57*, 20240046. [CrossRef]
2. Alam, K.H.; Rohen, Y.; Tomar, A.; Sajid, M. On geometry of fixed figures via φ-interpolative contractions and application of activation functions in neural networks and machine learning models. *Ain Shams Eng. Journal* **2025**, *16*, 103182. [CrossRef]
3. Berinde, V. Picard iteration converges faster than Mann iteration for a class of quasi-contractive operators. *Fixed Point Theory Appl.* **2004**, *2*, 97–105. [CrossRef]
4. Mann, W.R. Mean value methods in iteration. *Proc. Amer. Math. Soc.* **1953**, *4*, 506–510. [CrossRef]
5. Ishikawa, S. Fixed points by a new iteration method. *Proc. Am. Math. Soc.* **1974**, *44*, 147–150. [CrossRef]
6. Noor, M.A. New approximation schemes for general variational inequalities. *J. Math. Anal. Appl.* **2000**, *251*, 217–229. [CrossRef]
7. Alam, K.H.; Rohen, Y.; Saleem, N.; Aphane, M.; Razzaque, A. Convergence of Fibonacci–Ishikawa iteration procedure for monotone asymptotically non-expansive mappings. *J. Inequalities Appl.* **2024**, *2024*, 81. [CrossRef]
8. Alam, K.H.; Rohen, Y. An efficient iterative procedure in hyperbolic space and application to non-linear delay integral equation. *J. Appl. Math. Comput.* **2024**, *70*, 429–4317. [CrossRef]
9. Alam, K.H.; Rohen, Y. Convergence of a refined iterative method and its application to fractional Volterra–Fredholm integro-differential equations. *Comput. Appl. Math.* **2025**, *44*, 2. [CrossRef]
10. Ofem, A.E.; Igbokwe, I.D. An efficient Iterative method and its applications to a nonlinear integral equation and delay differential equation in Banach space. *Turk. J. Inequalities* **2020**, *4*, 79–107.
11. Kang, S.; Nazeer, W.; Tanveer, M.; Shahid, A. New fixed point results for fractal generation in Jungck Noor orbit with s-convexity. *J. Funct. Spaces* **2015**, *2015*, 963016. [CrossRef]
12. Nazeer, W.; Kang, S.; Tanveer, M.; Shahid, A. Fixed point results in the generation of Julia and Mandelbrot sets. *J. Inequalities Appl.* **2015**, *2015*, 298. [CrossRef]
13. Mishra, M.; Ojha, D.; Sharma, D. Some common fixed point results in relative superior Julia sets with Ishikawa iteration and s-convexity. *Int. J. Adv. Eng. Sci. Technol.* **2011**, *2*, 175–180.
14. Cho, S.; Shahid, A.; Nazeer, W.; Kang, S. Fixed point results for fractal generation in Noor orbit and s-convexity. *SpringerPlus* **2016**, *5*, 1843. [CrossRef]
15. Kumari, S.; Kumari, M.; Chugh, R. Generation of new fractals via SP orbit with s-convexity. *Int. J. Eng. Technol.* **2017**, *9*, 2491–2504. [CrossRef]
16. Gdawiec, K.; Shahid, A. Fixed point results for the complex fractal generation in the S-iteration orbit with s-convexity. *Open J. Math. Sci.* **2018**, *2*, 56–72. [CrossRef]
17. Orsucci, F. *Complexity Science, Living Systems, and Reflexing Interfaces: New Models and Perspectives*; IGI Global: Hershey, PA, USA, 2012.
18. Sreenivasan, K.R. Fractals and multifractals in fluid turbulence. *Annu. Rev. Fluid Mech.* **1991**, *23*, 539–604. [CrossRef]
19. Kenkel, N.C.; Walker, D.J. Fractals in the biological sciences. *Coenoses* **1996**, *11*, 77–100.
20. Devaney, R.L. *A First Course in Chaotic Dynamical Systems: Theory and Experiment*, 2nd ed.; Addison-Wesley: Boston, MA, USA, 1992.
21. Mandelbrot, B.B. *The Fractal Geometry of Nature*; W. H. Freeman: New York, NY, USA, 1982.
22. Barnsley, M. *Fractals Everywhere*, 2nd ed.; Academic Press: San Diego, CA, USA, 1993.
23. Julia, G. Mémoire sur l'itération des fonctions rationnelles. *J. Math. Pures Appl.* **1918**, *8*, 47–745.
24. Fisher, Y. Fractal image compression. *Fractals* **1994**, *2*, 347–361. [CrossRef]
25. Cohen, N. Fractal antenna applications in wireless telecommunications. In Proceedings of the Professional Program Proceedings. Electronic Industries Forum of New England, Boston, MA, USA, 6–8 May 1997; pp. 43–49.
26. Liu, S.A.; Bai, W.L.; Liu, G.C.; Li, W.H.; Srivastava, H.M. Parallel fractal compression method for big video data. *Complexity* **2018**, *2018*, 2016976. [CrossRef]

27. King, C.C. Fractal and chaotic dynamics in nervous systems. *Prog. Neurobiol.* **1991**, *36*, 279–308. [CrossRef]
28. Martinez, F.; Manriquez, H.; Ojeda, A.; Olea, G. Organization Patterns of Complex River Networks in Chile: A Fractal Morphology. *Mathematics* **2022**, *10*, 1806. [CrossRef]
29. Dhurandhar, S.V.; Bhavsar, V.C.; Gujar, U.G. Analysis of z-plane fractal images from $z \rightarrow z\alpha+c$ for $\alpha<0$. *Comput. Graph.* **1993**, *17*, 89–94.
30. Adhikari, N.; Sintunavarat, W. Exploring the Julia and Mandelbrot sets of $z^p+\log c^t$ using a four-step iteration scheme extended with s-convexity. *Math. Comput. Simul.* **2024**, *220*, 357–381. [CrossRef]
31. Griffin, C.; Joshi, G. Octonionic Julia sets. *Chaos Solitons Fractals* **1992**, *2*, 11–24. [CrossRef]
32. Singh, S.; Jain, S.; Mishra, S. A new approach to superfractals. *Chaos Solitons Fractals* **2009**, *42*, 3110–3120. [CrossRef]
33. Kumari, S.; Gdawiec, K.; Nandal, A.; Postolache, M.; Chugh, R. A novel approach to generate Mandelbrot sets, Julia sets and biomorphs via viscosity approximation method. *Chaos, Solitons Fractals* **2022**, *163*, 112540. [CrossRef]
34. Rani, M.; Kumar, V. Superior Julia set. *J. Korea Soc. Math. Educ. Ser. D Res. Math. Educ.* **2004**, *8*, 261–277.
35. Chauhan, Y.S.; Rana, R.; Negi, A. New Julia sets of Ishikawa iterates. *Int. J. Comput. Appl.* **2010**, *7*, 34–42. [CrossRef]
36. Li, D.; Tanveer, M.; Nazeer, W.; Guo, X. Boundaries of filled Julia sets in generalized Jungck-Mann orbit. *IEEE Access* **2019**, *7*, 76859–76867. [CrossRef]
37. Antal, S.; Tomar, A.; Prajapati, D.J.; Sajid, M. Variants of Julia and Mandelbrot sets as fractals via Jungck-Ishikawa fixed point iteration system with s-convexity. *AIMS Math.* **2022**, *7*, 10939–10957. [CrossRef]
38. Alam, K.H.; Rohen, Y.; Saleem, N.; Aphane, M.; Razzaque, A. On escape criterion of an orbit with s-convexity and illustrations of the behavior shifts in Mandelbrot and Julia set fractals. *PLoS ONE* **2025**, *20*, e0312197, *in press*. [CrossRef]
39. Jungck, G. Commuting mappings and fixed points. *Am. Math. Mon.* **1976**, *83*, 261–263. [CrossRef]
40. Chugh, R.; Kumar, V. Strong Convergence and Stability results for Jungck–SP iterative scheme. *Int. J. Comput. Appl.* **2011**, *36*, 40–46.
41. Olatinwo, M.O.; Imoru, C.O. Some convergence results for the Jungck–Mann and the Jungck–Ishikawa iteration processes in the class of generalized Zamfirescu operators. *Acta Math. Univ. Comen. New Ser.* **2008**, *27*, 299–304.
42. Hussain, N.; Kumar, V.; Kutbi, M.A. On rate of convergence of Jungck-type iterative schemes. *Abstr. Appl. Anal.* **2013**, *2013*, 132626. [CrossRef]
43. Guran, L.; Shabbir, K.; Ahmad, K.; Bota, M.F. Stability, Data Dependence, and Convergence Results with Computational Engendering of Fractals via Jungck–DK Iterative Scheme. *Fractal Fract.* **2023**, *7*, 418. [CrossRef]
44. Jungck, G.; Hussain, N. Compatible maps and invariant approximations. *J. Math. Anal. Appl.* **2007**, *325*, 1003–1012. [CrossRef]
45. Singh, S.L.; Bhatnagar, C.; Mishra, S.N. Stability of Jungck-type iterative procedures. *Int. J. Math. Math. Sci.* **2005**, *19*, 3035–3043. [CrossRef]
46. Weng, X. Fixed point iteration for local strictly pseudo contractive mapping. *Proc. Amer. Math. Soc.* **1991**, *113*, 727–731. [CrossRef]
47. Pinheiro, M. s-convexity: Foundations for analysis. *Differ. Geom. Dyn. Syst.* **2008**, *10*, 257–262.